

An Experimentally Validated Thermo-Mechanical Finite Element Model for Friction Stir Welding in Carbon Steels

A. H. Kheireddine, A. A. Khalil, A. H. Ammouri, G. T. Kridli, and R. F. Hamade

Abstract—Solidification cracking and hydrogen cracking are some defects generated in the fusion welding of ultrahigh carbon steels. However, friction stir welding (FSW) of such steels, being a solid-state technique, has been demonstrated to alleviate such problems encountered in traditional welding. FSW include different process parameters that must be carefully defined prior processing. These parameters included but not restricted to: tool feed, tool RPM, tool geometry, tool tilt angle. These parameters form a key factor behind avoiding warm holes and voids behind the tool and in achieving a defect-free weld. More importantly, these parameters directly affect the microstructure of the weld and hence the final mechanical properties of weld. For that, 3D finite element (FE) thermo-mechanical model was developed using DEFORM 3D to simulate FSW of carbon steel. At points of interest in the joint, tracking is done for history of critical state variables such as temperature, stresses, and strain rates. Typical results found include the ability to simulate different weld zones. Simulations predictions were successfully compared to experimental FSW tests. It is believed that such a numerical model can be used to optimize FSW processing parameters to favor desirable defect free weld with better mechanical properties.

Keywords—Carbon Steels, DEFORM 3D, FEM, Friction stir welding.

I. INTRODUCTION

FRICTION stir welding (FSW) is a relatively new technique used for joining similar or dissimilar metals using a nib or a pin inserted along the weld steam [1]. This technique is based on the massive plastic deformation of the joined metals without subjecting them to any form of induced heating or melting. During the welding process, the material is wiped from the front side of the nib onto the back side in a helical motion within the stir zone [2].

Friction stir welding has its advantages over other welding techniques. It enables an efficient control on the cooling rate and peak temperature by varying the speed of rotation of the nib [3]. FSW is significantly useful for metals with poor weldability due to its solid-state joining nature, in addition to being used in many green applications that aim at saving the environment and the energy consumption as well [4]. Friction stir welding is mostly used in aerospace industry to join high

strength aluminum alloys that are hard to weld using traditional welding techniques. For steel and other high-temperature materials, the application of FSW is limited to the presence of suitable tools that can operate in the temperature range of 1000 to 1200°C [5]. This is due to the fact that the heat produced by stirring and friction is not sufficient to soften the material around the rotating tool. Therefore, it is important to select tool materials with good wear resistance and toughness at temperatures of 1000°C or higher [4]. However, in the past five years, studies have reported that FSW achieves similar grain improvements in the stir zone of steels similar to the ones observed for aluminum.

The microstructure and mechanical properties of carbon steel joints are significantly affected by the following factors: heat input during welding, the composition of steel metal used and the processing history of the welded base material [7]. FSW has a significant role in refinement of ferrite and austenite phases through dynamic recrystallization. In turn the small sized grains obtained increase the hardness and strength of the stir zone, and as a result, weld transverse tensile failures consistently occur near the border of the stir zone, thus exhibiting almost the same yield and ultimate tensile strengths as the base material [8]. For high carbon steels the lower welding speed can also form strong joints consisting of a refined two-phase structure consisting of ferrite and pearlite by preventing martensite formation due to the lower cooling rate. The lower heat inputs in FSW are expected to minimize the distortion and the residual stresses in steels enhancing the ability to weld thick components together. This adds to the ability of FSW to eliminate the weld fumes and the problems caused by hydrogen cracking in steels due to the solid-state nature of FSW process [4]. Sun et al. studied the effect of laser preheating on the welding parameters, final microstructure and mechanical properties of the joints in S45C steel. The experimental results show the effect of laser beam on increasing the welding speed of FSW in S45C steel. [9].

Huge efforts nowadays are spent on optimizing and enhancing FSW. Traditional experimental methods are believed to be time and money consuming. But in the last decade many researches numerically simulated FSW for prediction and optimization proposes. Early models of the friction stir processes used thermal models to simulate the heat generation in the process. More accurate coupled thermo-mechanical models were introduced afterwards using several commercial software such as DEFORM [10] and ABAQUS [11].

A. H. Kheireddine, A. A. Khalil, A. H. Ammouri, and R. F. Hamade are with the Department of Mechanical Engineering, American University of Beirut (AUB), Beirut, Lebanon.

G. T. Kridli is with the Department of Industrial and Manufacturing Systems Engineering, University of Michigan, Dearborn, Michigan USA.

(A. H. Kheireddine, corresponding author, e-mail: ahk26@aub.edu.lb).

Most of the developed models tackled FSW of lightweight materials. Very little work was done on simulating FSW in steels. In [6] Cho et al. used an Eulerian formulation to simulate coupled viscoplastic flow and heat transfer around the tool pin. This work the influence of the welding parameters on material flow and the shape of the interface between the various zones in friction stir welding of stainless steel (304L) [6].

In this paper, a 3D fully thermo-mechanically coupled FE model was developed to simulate the Friction stir welding of carbon steel. The model was validated against experimental data.

II. THE FE MODEL

A. Parts & Meshes

A thermo-mechanically coupled model using the FE software DEFORM was implemented to model the friction stir welding of steel. As shown in Fig. 2, the model comprises the tool, the workpiece, and the backing plate.

Both the tool and the backing plate were modeled as rigid un-deformable bodies where only heat transfer was accounted. On the other hand the workpiece was modeled as a plastic body subject to deformation and heat. The two plates to be welded were modeled as one block to avoid numerical instabilities at the contact.

The considered tool was a cylindrical shoulder 15mm in diameter. From the bottom of the shoulder, a 6mm diameter smooth unthreaded pin extrudes 3.2mm. The tool was tilted 3° about the vertical axis in the processing direction to further improve material flow. Both the workpiece and the backing plate had an area of 60x40mm² and a thickness of 3.2mm.

Tetrahedral elements were used in the FEM model. The tool and the backing plate were meshed for thermal analysis purposes only with each containing around 10000 and 5000 elements respectively while the workpiece had around 24000 elements. To further capture the state variables at the tool-workpiece interface, a rectangular mesh control window was applied around the processing area of interest where finer mesh elements (around 0.6mm) were created as shown in Fig. 1.

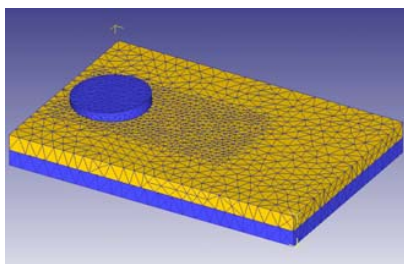


Fig. 1 The meshed FE model showing the tool, workpiece and backing plate

B. Material

The material used for the tool and the backing plate was WC based alloy. As for the workpiece, the material used was AISI 1045. Constant mechanical properties of

AISI1045 defined in the model are shown in Table I. Moreover, as per DEFORM recommendation, all other material properties were defined as a function of temperature. A thermo- visco-plastic was used to formulate the stress in AISI1045. Specifically, the generalized Oxley's equation was used as follows:

$$\sigma = \sigma_1(T_{mod}) (\dot{\epsilon}^P)^{n(T_{mod})} \quad (1)$$

$$T_{mod} = T(1 - \nu \log_{10} \frac{\dot{\epsilon}^P}{\dot{\epsilon}_0^P}) \quad (2)$$

where

σ = Flow stress

T = Material temperature

T_{mod} = Modified temperature

$\dot{\epsilon}^P$ =Plastic strain

$\dot{\epsilon}_0^P$ = Plastic strain rate

$\dot{\epsilon}_0^P$ = Reference plastic strain rate

ν = Strain rate sensitivity constant

σ_1, n = polynomial functions

TABLE I
MATERIAL PROPERTIES

Property	Value
Elastic Modulus [11]	44830 MPa
Poisson's ratio [11]	0.35
Coefficient of thermal expansion [11]	2.65×10^{-5}
Thermal conductivity [11]	96 N/(s K)
Heat capacity [12]	2.43 N/(mm ² C)
Emissivity [12]	0.12
Material constant A [13]	27.5 s^{-1}
Material constant α [13]	0.052 MPa^{-1}
Activation energy ΔH [13]	130 kJ/mol
Material constant n [13]	1.8
Universal gas constant R [13]	8.314 J/(kg K)
Property	Value
Poisson's ratio	0.3
Emissivity	0.75

C. Boundary & Friction Conditions

Heat transfer with the environment was accounted for all the three meshed objects with a convective heat coefficient of 20W/(m²°C) at a constant temperature of 293K. The heat transfer coefficient between the tool-workpiece and the backing plate-workpiece interfaces was set to 11kW/(m² °C).

Friction at the tool-workpiece interface is a very complex process due to the variation of temperature, strain rate, and stress which make friction modeling a difficult technique. The value of the friction coefficient (0.37) was used based on the following formula: [12]

$$\mu_r = \mu_0 \exp(-\lambda \delta \omega r) \quad (3)$$

where δ is the percentage sticking and r is the radial distance from the tool axis for the point in consideration.

The values taken were as follows: $\mu_0 = 0.4$, $\delta = 0.4$, $\omega = 62.8$ radians, $r = 0.003\text{m}$ and constant λ was 1s/m [13].

Local re-meshing was triggered by a relative interference ratio of 70% between contacting edges. This would ensure the integrity of the workpiece geometry during deformation.

The simulation time step selection should be optimized to prevent redundant calculations while preserving the state variables' accuracy. The time step in the simulation was calculated based on the tool rotational speed and the minimum element size to guarantee a calculation step every 5 degrees of the tool rotation.

Simulation time was further reduced by neglecting the plunging phase of FSW and taking into consideration the traversing phase alone. The tool final plunged shape was cut from the workpiece geometric model to account for the deformation produced by the plunging phase. A dwelling phase was added at the beginning of each run where the tool rotates in its place to raise the temperature at the stir zone to the plunging elevated levels.

In tool movement definition a trapezoidal speed profile with a rise time of 0.5 sec was used. This would ensure a smooth processing start and prevent voids at the plunging region.

III. RESULTS

A. Model Validation

The FEM model was validated with experimental data available in the literature by tracking the temperature history of an observation point on the traverse line at a distance of 0.5mm above the shoulder for two different test cases. The processing parameters of these cases are described in Table II.

Property	Case 1	Case 2
Rotational speed (RPM)	100	400
Traverse speed (mm/min)	100	100

From Fig. 2 we can observe a comparison between the simulated temperatures and measured peak temperature for case 2. It can be seen that the peak simulated temperature is very close to the experimentally measured maximum temperature. A similar comparison was made for case 2 and matching results were reached as shown in Fig. 3.

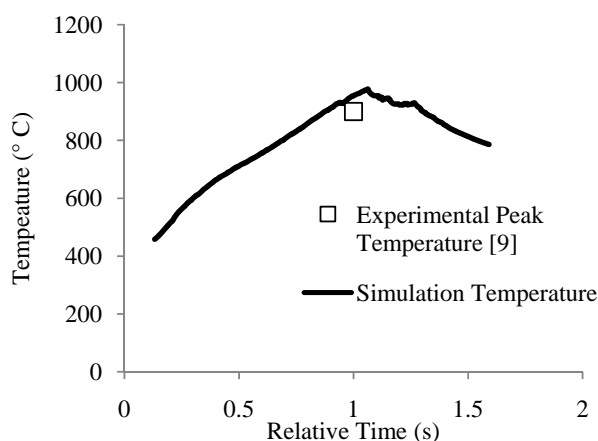


Fig. 2 Simulation Temperature Profile with experimental peak temperature

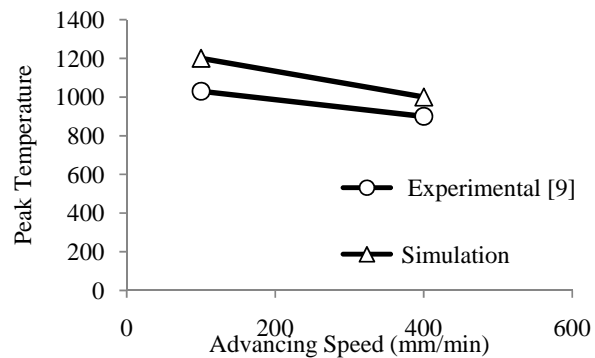


Fig. 3 Peak temperature versus advancing speed for experimental and simulation test cases

B. Effect of Advancing Speed on Temperature

The effect of the tool advancing speed on the weld temperature was studied. It was found that as the advancing speed increases the welding temperature decreases. This trend is reached experimentally and through the simulation as shown in Fig. 3.

1. Strain Distribution

Another important parameter extracted from the developed FE model was the effective strain. It is shown from Fig. 4 that the strain reaches maximum value at the weld centre and decreases as we move away from the weld line. Moreover, the strains on the advancing side of the weld are higher which proves the non-symmetry property of the FSW welds. Moreover, also from Fig. 4, the value of the strain decreases with increasing advancing speed.

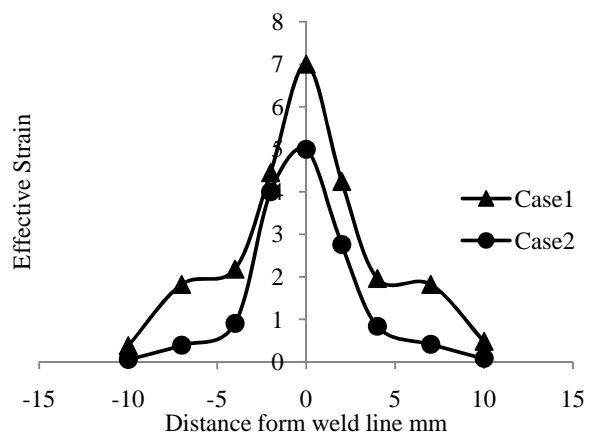


Fig. 4 Effective strain distribution across the weld section for both test cases

IV. CONCLUSIONS

The developed thermo-mechanical FE model in this work was able to successfully simulate the FSW process and was validated with previous experimental work by other researchers. The effect of advancing speed on temperature and

strain distribution of the weld was analysed. It was reached that with higher advancing speeds lower strains can be reached in the weld but with lower temperatures also. It is believed that such model can be used for later optimization purposes.

ACKNOWLEDGMENTS

This publication was made possible by a National Priorities Research Program grant from the Qatar National Research Fund (a member of The Qatar Foundation). The statements made herein are solely the responsibility of the authors.

REFERENCES

- [1] T. Lienert, W. Stellwag, JR., B. Grimmer, R. Warke. 2003. Friction Stir Welding Studies on Mild Steel. Supplement to the welding journal (1-S-9-S)
- [2] M. Guerra, C. Schmidt, J.C. McClure, L.E. Murr, A.C. Nunes, 2002. Flow patterns during friction stir welding. *Materials Characterization* 49 (2003) 95–101. Department of Metallurgical and Materials Engineering, University of Texas at El Paso, El Paso, TX 79968-0520, USA NASA, Marshall Space Flight Center, Huntsville, AL, USA
- [3] L. Cui, H. Fujii, N. Tsuji, K. Nogi. 2007. Friction stir welding of a high carbon steel. *Scripta Materialia* 56 (2007) 637–640. Joining and Welding Research Institute, Osaka University, 11-1 Mihogaoka, Ibaraki, Osaka 567-0047, Japan Department of Adaptive Machine Systems, Osaka University, Suita, Osaka 565-0871, Japan
- [4] R. Mishra, Z. Ma. 2005. Friction stir welding and processing. *Materials Science and Engineering R* 50 (2005) 1–78 Center for Friction Stir Processing, Department of Materials Science and Engineering, University of Missouri, Rolla, MO 65409, USA Institute of Metal Research, Chinese Academy of Sciences, Shenyang 110016, China
- [5] A. Ozekcin, H. Jin, J. Koo, N. Bangaru, R. Ayer. 2004. A Microstructural Study of Friction Stir Welded Joints of Carbon Steels. *International Journal of Offshore and Polar Engineering*.
- [6] J. Cho, Donald E. Boyce, P. Dawson. 2005. Modeling strain hardening and texture evolution in friction stir welding of stainless steel. *Materials Science and Engineering A* 398 (2005) 146–163. Sibley School of Mechanical and Aerospace Engineering, Cornell University, 196 Rhodes Hall, Ithaca, NY 14853, USA
- [7] H. Fujii, L. Cui, N. Tsuji, M. Maeda, K. Nakata, K. Nogi. 2006. Friction stir welding of carbon steels. *Materials Science and Engineering A* 429 (2006) 50–57. Joining and Welding Research Institute, Osaka University, 11-1 Mihogaoka, Ibaraki, Osaka 567-0047, Japan. Department of Adaptive Machine Systems, Osaka University, Suita, Osaka 565-0871, Japan, Center for Advanced Science and Innovation, Osaka University, Suita, Osaka 565-0871, Japan
- [8] Y. Sato, T. Nelson, C. Sterling, R. Steel, C. Pettersson. 2005. Microstructure and mechanical properties of friction stir welded SAF 2507 super duplex stainless steel. *Materials Science and Engineering A* 397 (2005) 376–384. Department of Materials Processing, Graduate School of Engineering, Tohoku University, 6-6-02 Aramaki-aza-Aoba, Sendai 980-8579, Japan Mechanical Engineering Department, Brigham Young University, 435 CTB, Provo, UT 84602, USA MegaStir Technologies, 275 West 2230 North, Provo, UT 84604, USA Sankvik Materials Technology, Sandviken S-811 81, Sweden
- [9] Y. Sun, Y. Konishi, M. Kamai, H. Fujii. Microstructure and mechanical properties of S45C steel prepared by laser-assisted friction stir welding. *Materials and Design* 47 (2013) 842–849. Joining and Welding Research Institute, Osaka University, Japan
- [10] Buffa, G., Fratini, L., and Shivpuri, R., 2007, "CDRX Modelling in Friction Stir Welding of AA7075-T6 Aluminum Alloy: Analytical Approaches," *Journal of Materials Processing Technology*, 191(1-3) pp. 356-359.
- [11] H. R. Mackenzie, D., and Li, H., 2010, "Multi-Physics Simulation of Friction Stir Welding Process," *Engineering Computations* (Swansea, Wales), 27(8) pp. 967-985.
- [12] Nandan, R., Prabhu, B., De, A., & Debroy, T. (2007). Improving reliability of heat transfer and materials flow calculations during friction stir welding of dissimilar aluminum alloys. *WELDING JOURNAL-NEWYORK*, 86(10), 313.
- [13] Nandan, R., Roy, G. G., Lienert, T. J., & Debroy, T. (2007). Three-dimensional heat and material flow during friction stir welding of mild steel. *Acta Materialia*, 55(3), 883-895.